Identification of the Zero-g Shape of a Space Beam

Gary J. Balas* and Charles D. Babcock†
California Institute of Technology, Pasadena, California

An approach for identifying the 0-g shape of a beam/column in a 1-g environment is developed. The determination of the 0-g shape is accomplished by a combination of experiment and analysis. A prototype large space structure beam/column is scaled to laboratory size to demonstrate that the 0-g shape of the structure can be determined accurately in a ground-based experiment. Information obtained from the 0-g-shape experiment also is used to experimentally measure the stiffness of the beam model.

Nomenclature

A	= area
E	= Young's modulus
F	= force
F_a, F_b, F_c	= forces at supports
g	= gravity
I	= moment of inertia
l	= length of beam
L	= length
n	= number of bays
T	= time
v_a, v_b	= Bernoulli-Euler beam deflections
θ	= crossbracing angle
ρ	= density (weight/volume)
ω_{ex}	= experimentally determined shape
ω_{0-g}	= 0-g shape

Subscripts

p	= prototype
m	= experimental model

Introduction

IN the past, aerospace structural systems have been subject to some form of structural verification prior to flight. The verification procedure usually includes experimental testing to ensure that the structure can carry the design loads and be within specified deflections. For these space structures, the launch loads were the driving criterion for design. The launch loads generated deflections that usually were greater than the 1-g induced deflections. Therefore, testing in a 1-g environment posed no special problems.

Space structures of the future present unique problems for system designers. These structures will require some means of deployment, assembly, or fabrication in space, an environment for structures that is quite benign. Such structures will not be subject to launch loads that previous structures have had to endure and the applied loads are apt to be small compared to 1-g loads. In addition, some space structures, such as large antennas, must be built very accurately. Missions envisioned for large antennas involve diameter-to-wavelength ratios of around 1,000 and up to 100,000, including ones for which the main beam must contain almost all the radiated energy. This requires that the emitted wave front be accurate to within 4% of the wavelength. These constraints lead to a surface error requirement of between 1/1,000th and 1/100,000th of the diameter of the antenna.[1] Hence, structural imperfections are of major importance.

The important aspect of the problem is that these structures will have to operate in a 0-g environment. Therefore, it is necessary to identify the structural shape that will occur in a 0-g environment. Projects that use deployable structures in space consistently have been tested on the ground because of the economic advantage of such tests and the ability to modify the design before flight. Consequently, there is a need to develop tests to determine 0-g properties of these structures while on Earth.

Large space structures will be designed to operate only in space and will not be designed to operate at 1-g, since it is not required for their function. In order to determine the 0-g properties in a 1-g environment, these structures must be deployed or erected along with being artificially supported. This introduces constraints into the shape of the structure in the 1-g environment that can be difficult to quantify.

This paper looks at one such problem for the structural part of a typical large space structure—a beam/column. It is demonstrated that the 0-g shape of the structure can be determined accurately in a ground-based environment by a combination of experiment and analysis. The process is as follows: The structure is supported in a redundant manner, with the load at each support determined experimentally. The shape of the structure under these loads is then measured. This shape includes the 0-g shape, measurement offset, and the deflection under the known loads (gravity loads and support loads). A straightforward analysis determines the 0-g shape.

This process is displayed pictorially in Fig. 1. The space structure is supported by a support system F and is loaded by gravity. The shape, ω_{ex}, is measured. L represents the structural operator (i.e., stiffness matrix). The initial shape, $\omega_{0\text{-}g}$, is found by the operation indicated in the figure. The theoretical concepts of these operations are straightforward but implementation may pose many numerical difficulties.

This procedure is demonstrated using a beam/column scaled to laboratory size. A series of experiments is performed on the beam model. Two objectives are pursued using the experimental data. The first identifies the 0-g shape of the beam model. The second, assuming the 0-g shape is constant, derives the stiffness of the beam model. Discussion of the scaling, analysis, experimental setup, experiments, and results is given in the following sections.

Presented as Paper 87-0872 at the AIAA/ASME/ASCE/AHS 28th Structures, Structural Dynamics and Materials Conference, Monterey, CA, April 6-8, 1987; received April 14, 1988; revision received July 5, 1988.

*Graduate Research Assistant, Graduate Aeronautical Laboratories. Member AIAA.

†Professor of Aeronautics and Applied Mechanics, Graduate Aeronautical Laboratories. Member AIAA. (He is now deceased.)

Analysis

A relationship between the measurement of the shape of a space beam/column in a 1-g environment and its 0-g shape needs to be established. The beam/column will be referred to as beam in the following discussion. Assuming an ideal Bernoulli-Euler beam, its deflection is calculated under its own weight and support conditions. The difference between the measured shape of the beam and the deflection of the Bernoulli-Euler beam with its support conditions provides the 0-g shape of the beam.

For an experiment, a driving criterion is to have the deflection caused by gravity be on the same order or less than its imperfections. This allows the deflection sensor to accurately measure the imperfection and the deflection due to gravity. At first, an analytical model of the beam was examined with two end supports. The deflection of the analytical beam model under a 1-g loading was of an order of magnitude greater than the initial assumed imperfections. Redundant supports allow more accurate determination of the 0-g shape of structures since 1-g induced deflections are reduced. (Large space structures, in general, are flimsy in a 1-g environment and will require redundant supports to prevent sizable deformation.) Therefore, a beam supported at three places (one redundant middle support) was analyzed and showed a 1:5 ratio of the 1-g deflection to an assumed initial imperfection. This beam support system is used in the analysis and experiment. The experimental setup is shown in Fig. 2.

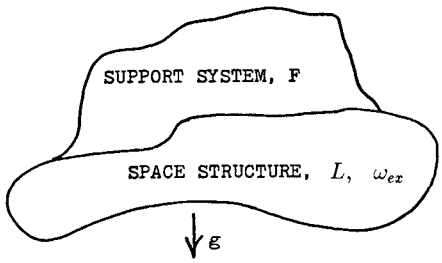

- MEASURE SUPPORT SYSTEM LOADS, F
- MEASURE SPACE STRUCTURE CONFIGURATION, ω_{ex}
- CALCULATE SPACE STRUCTURE SHAPE UNDER 0-g, ω_{0-g}

$$L(\omega_{ex} - \omega_{0-g}) = F + mg$$

$$\omega_{0-g} = \omega_{ex} - L^{-1}(F + mg)$$

Fig. 1 Zero-g shape determination.

The 1-g deflection of the analytical beam model is calculated as follows: The equation of a linear elastic, homogeneous material beam with a constant EI and three supports can be written as

$$EI(\omega_{ex} - \omega_{0\text{-}g})'''' = -\rho gA + F_a\delta(x) + F_b\delta(x - 2l) + F_c\delta(x - 4l) \quad (1)$$

The function $EI(\cdot)''''$ is a linear operator and is labeled L. Taking the inverse of L

$$\omega_{ex} - \omega_{0\text{-}g} = L^{-1}[-\rho gA + F_a\delta(x) + F_b\delta(x - 2l) + F_c\delta(x - 4l)] \quad (2)$$

which leads to

$$\omega_{ex} = \omega_{0\text{-}g} - L^{-1}[-\rho gA + F_a\delta(x) + F_b\delta(x - 2l) + F_c\delta(x - 4l)] \quad (3)$$

The following conditions are satisfied in the analysis as a result of overall equilibrium:

$$F_a + F_b + F_c = 4\rho gAl \quad \text{and} \quad F_a = F_c \quad (4)$$

The deflection of the model, ω_{ex}, is measured from the experiment. The deflection of the ideal Bernoulli-Euler beam needs to be determined. The beam is modeled analytically with the conditions as shown in Fig. 3. The analytical beam model is divided into beams A and B, which have two different x axes for simplicity. At point a, the boundary conditions are zero displacement, by definition, and zero moment. At point b, the deflection, slope, and moment must be equal to the same quantities on both sides, and the shear force on the positive side must be equal to the shear force plus F_b on the negative side. Point c has the same boundary conditions as point a. These boundary conditions lead to the following equations, where v_i are the beam's deflections.

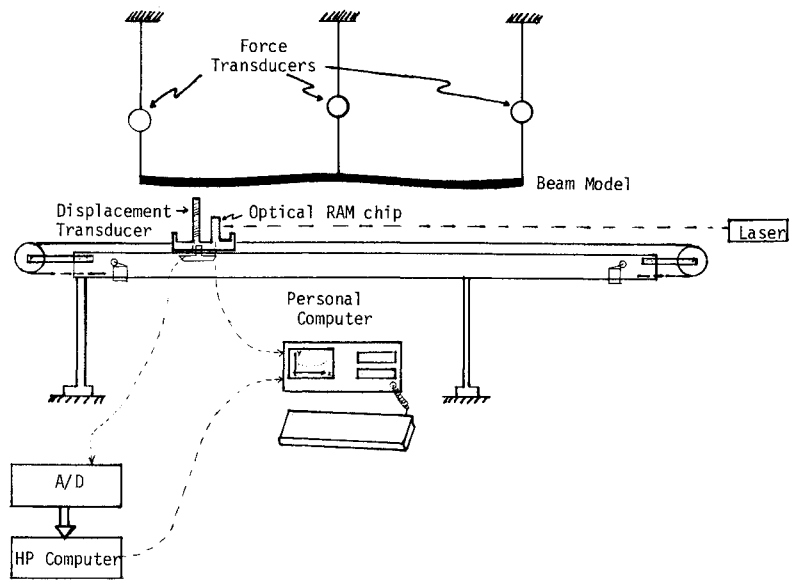

Fig. 2 Experimental setup of beam model.

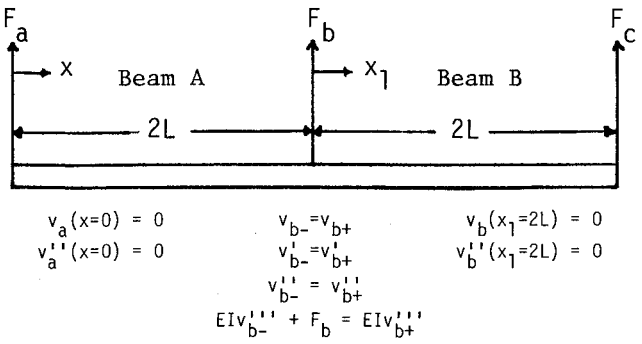

Fig. 3 Analysis model of the beam.

Beam A:

$$v_A = \frac{1}{EI}\left\{\frac{-\rho g A x^4}{24} + \left(2\rho g A l - \frac{1}{2}F_b\right)\frac{x^3}{6} + \left(F_b l^2 - \frac{8}{3}\rho g A l^3\right)x\right\} \tag{5}$$

Beam B:

$$v_B = \frac{1}{EI}\left\{\frac{-\rho g A x_1^4}{24} + \frac{F_b x_1^3}{12} + (2\rho g A l^2 - F_b l)\frac{x_1^2}{2} + \frac{4}{3}F_b l^3 - \frac{10}{3}\rho g A l^4\right\} \tag{6}$$

The 0-g shape of beams A and B now can be found with the following equations:

Beam A:

$$\omega_{0\text{-}g}\,|_{0\le x\le 2l} = \omega_{ex}\,|_{0\le x\le 2l} - v_a \tag{7}$$

Beam B:

$$\omega_{0\text{-}g}\,|_{2l\le x\le 4l} = \omega_{ex}\,|_{2l\le x\le 4l} - v_b, \qquad x_1 = x - 2l \tag{8}$$

The equations for beams A and B satisfy the boundary conditions imposed and take into consideration the rigid-body displacements and rotations. In the analysis, the x axis is taken to be between the ends of the beam, which specifies the rigid-body translations and rotation.

Experimental Verification

Structural Scaling

Scaling provides a way of experimentally testing a model of a structural system that will have the same behavior as the prototype structure. The prototype structure is a beam/column envisioned to be part of a large space structure. The desired quantity of interest is the initial shape of a space beam in 0-g. The parameters of a beam/column are listed in Table 1.

Using Buckingham's II rule, there are six parameters and three dimensions, which leads to three dimensionless quantities. These dimensionless quantities and necessary scaling conditions for the experimental model and prototype are as follows:

$$\left(\frac{a}{l}\right)_p = \left(\frac{a}{l}\right)_m = \frac{L}{L} \tag{9}$$

$$\left(\frac{Pl^2}{EI}\right)_p = \left(\frac{Pl^2}{EI}\right)_m = \frac{FL^2}{FL^2} \tag{10}$$

$$\left(\frac{m_g L^3}{EI}\right)_p = \left(\frac{m_g L^3}{EI}\right)_m = \frac{FT^2L^4}{FT^2L^4} \tag{11}$$

Table 1 Prototype beam/column parameters

Parameters	Units
Beam length, l	L
Bending stiffness, EI	FL^2
Mass/length, m	FT^2/L^2
Buckling load, P	F
Gravity, g	L/T^2
Initial deformation, a	L

Table 2 Column design parameters

Maximum load on the column	500 N
Length, l	50 m
Modulus, graphite epoxy	110.3×10^9 N/m^2
Crossbracing angle, θ	45 deg
Number of bays, n	125
Density, ρ	1522 kg/m^3

Table 3 Prototype and model specifications

Solid rod trust column	Steel bar
Prototype	Model
l = 50 m	l = 2 m
$E = 110.3 \times 10^9$ N/m^2	$E = 199.8 \times 10^9$ N/m^2
$I = 2.447 \times 10^{-6}$ m^4	$I = 5.42 \times 10^{-10}$ m^4
g = 9.81 m/s^2	g = 9.81 m/s^2
$m = M/l$ = 0.2135 kg/m	m $= M/l$ = 1.306 kg/m
ρ_p = 1522 kg/m^3	ρ_p = 7831 kg/m^3

The subscripts p and m refer to the prototype and experimental model, respectively. A prototype space beam/column is selected to analyze and scale down for an experiment. Design guidelines specified by Mikulas[2] are used to select such a column. The design procedures are based primarily on the selection of a design buckling load and an initial imperfection of the column. Column imperfections can result from a number of causes—such as, manufacturing, thermal gradients, and lateral accelerations.

A solid rod, three-legged truss column design is used as the prototype. A recommended design imperfection ratio of $a/l = 0.0025$ is selected. The other specifications for the column prototype are listed in Table 2.

The equation for the moment of inertia of a solid rod truss column is

$$I = Al/2n^2 \tan^2\theta \tag{12}$$

These requirements led to a column with the following parameters: width, 0.4 m; diameter of longerons, 6.3 mm; mass of beam, 10.67 kg; moment of inertia, 2.447×10^{-6} m^4; and load/buckling load, 0.533.

The scaling laws allow matching the behavior of the prototype column with a scale model. If the dimensionless quantities of Eqs. (9–11) are the same for the model and prototype, the behavior is the same (assuming all important parameters have been identified). First, a length scale of 25 is selected, which defines an experimental model, 2 m in length. The model material selected is steel and the cross-sectional shape is assumed to be rectangular. These specifications lead to the parameters listed in Table 3. A model height of 6.17 mm is derived from Eq. (11). Note that the deflection of the model is not affected by its width.

The experimental beam model selected is constructed of steel, with a height of 6.35 mm, width of 25.4 mm, and a

length of 2 m. In order to measure the initial imperfection of the beam model, it is supported at three points along the beam. The calculated maximum theoretical deflection with the three supports is on the order of 1 mm. With an assumed imperfection ratio of 0.0025, $a = 5$ mm, the ratio of the 1-g deflection of the model to the imperfection is approximately 5. This ratio provides ample separation between the imperfection and the 1-g deflection to allow accurate determination of the initial imperfections in the model.

It is desired to have a measurement error of $\leq 1\%$ of the maximum displacement and maximum force in order to obtain a 2% accuracy in the measured 0-g shape. These requirements dictated that the resolution of the displacement be valid down to ± 25 μm (± 1 mil) and the force transducer be accurate to within 5 g.

Measurement System Scaling

The purpose of this experiment is to determine the 0-g shape of a beam model from measurements in a 1-g environment. The previous section dealt with the prototype beam selection. Scaling laws provided the sizing of the model beam from the prototype beam. The next important issue to address is the scaling of the measurement devices.

There are three basic measuring devices used in the experiment: force transducers, a displacement transducer, and an optical sensor. The force transducers measure the force in the model's supports. The displacement transducer, a noncontacting type, measures the shape of the model in relation to a reference track. The track itself is not flat to the desired accuracy of ± 25 μm (± 1 mil); therefore, it too must be measured. An optical sensor, in conjunction with a laser, is used to determine the flatness of the reference track. All three devices would need to be scaled up for a prototype experiment.

The weight of the model is 2.5 kg, whereas the prototype would weigh 10.7 kg. The force transducers see a maximum load of half of the beam's weight, 1.25 and 5.35 kg, respectively. A 1% accuracy is desired in the force transducers, which would require the resolution of 10 g for the model and 50 g for the prototype. The model's force transducers were built in the laboratory and have a resolution of 2 g. For the prototype, force transducers are either available from commercial sources or can be built with the required accuracy. This specification is relatively easy to meet and exceed.

The expected maximum deflection of the model is on the order of 5 mm. The desired accuracy of the displacement transducer is ± 25 μm (± 1 mil). A Bentley Nevada 7200 series 11-mm proximity transducer system was used in the model experiment. The Bentley Nevada transducer is noncontacting, and operates by generating a high-frequency signal radiated by a coil in the probe tip into the observed material setting up eddy currents. The impedance of the coil, caused by the creation of the eddy currents, is detected by the proximeter electronics, which converts the impedance change into a dc output. The 11-mm proximity transducer system has a range of 5 mm and an accuracy of ± 25 μm, satisfying the 1% accuracy requirement.

The prototype beam/column will have a maximum deflection of 165 mm, leading to a desired resolution of the shape measurement device of 1.65 mm. A different type of noncontacting displacement transducer system would have to be used with the prototype beam. However, obtaining an accuracy of 1 mm and a range of 200 mm over a distance of 50 m is easily obtainable with conventional measuring techniques. One such method would use a Theodolite to measure the deflection of points on the prototype.

The optical sensing system is designed to measure the flatness of the reference track. This system assists the displacement transducer in providing the desired 1% accuracy of the measured beam deflection. Since the displacement transducer rides on a cart, the optical sensor measures its trajectory as the cart traverses the track. A laser beam is shown horizontal to the cart's path providing a horizontal reference. The model experiment uses a 200-μm-diam laser

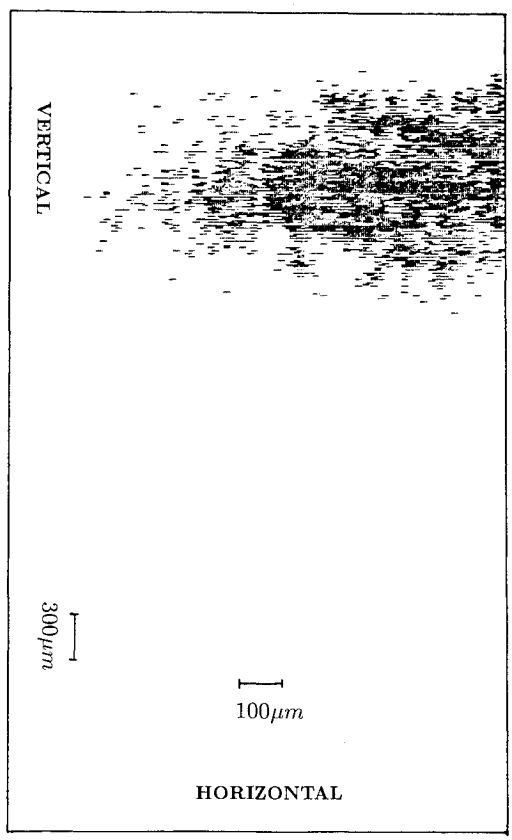

Fig. 4 Image of laser beam at point 1.

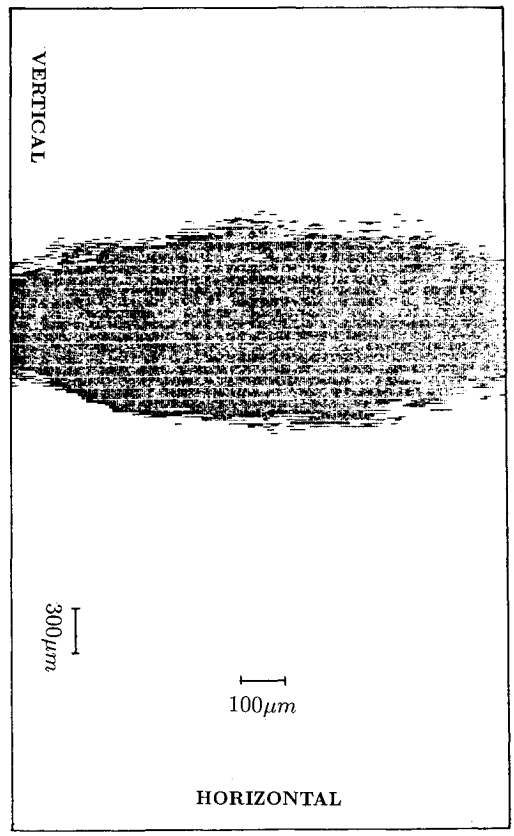

Fig. 5 Image of laser beam at point 51.

beam directed toward the optical sensor as the reference. The sensor is a dynamic RAM chip with an illumination area of 5.5×1.08 mm. Each pixel in the sensor measures 8×9 μm with the centers offset by 21 μm. The illuminated area is processed in a computer and provides a resolution of 21 μm in regards to the track's flatness. For the prototype, the track method of traversing a displacement transducer under the beam would not be appropriate. Therefore, it is not necessary to consider scaling up this measurement.

There are commercial instruments available today that would provide the accuracy required to measure the 0-g shape of large space structures in the Earth's environment. The methodology discussed requires both the 0-g experimental and analytical input. A discussion of the experiment follows.

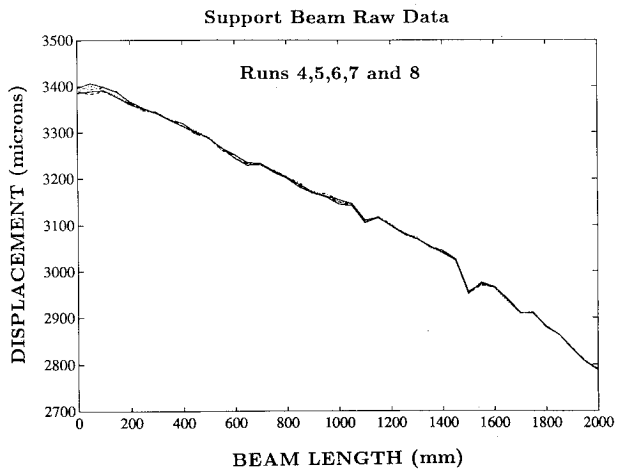

Fig. 6 Support beam displacement.

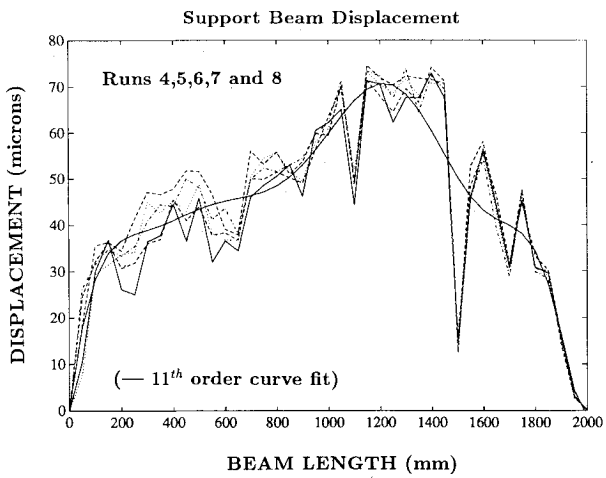

Fig. 7 Support beam displacement with bias removed.

Experimental Setup

The lab experiment consists of a 2-m beam model hung from three supports located at the middle and on either end of the beam. Its deflected shape is measured with a noncontacting displacement transducer, and in-line force transducers are used to measure the support reactions. A track is set up below the beam on which the measurement cart traverses. The measurement cart contains the noncontacting displacement transducer, light diode, and optical sensor. All of these devices provide information from which the 0-g shape of the beam model is determined. The experimental setup can be seen in Fig. 2.

Each in-line force transducer consists of a ring with four strain gages mounted on it, inside and outside. These gages are balanced through a bridge circuit. The gages are zeroed prior to each series of experiments and after turning over the beam model. The average drift in the gages is on the order of 0.02 mV or approximately 2 g. The forces in the supports can be varied via adjustment of turnbuckles, which are in-line with the force transducers. This allows for the deflection of the beam to be measured under a number of different load conditions.

The track consists of a 4-m steel I-beam, 12.70×7.62 mm, on which the measurement cart rides. The cart, connected by a cable and pulley system, is driven by a variable-speed motor. The variable-speed motor allows for the modification of the sample rate of data acquisition. The I-beam has two one-way limit switches mounted on it to allow the cart to be driven into and reversed out of the limit.

A light diode on the cart is used to trigger the analog-to-digital (A/D) converter and data acquisition system to take measurements. The light diode is placed above a black and silver strip taped to the center of the I-beam. It triggers the system to take a voltage reading from the displacement transducer when light is reflected into the diode. The tape used provides a data point every 5.08 mm (5 points/in.). The data acquisition system stores the information from the displacement transducer for off-line processing.

The displacement transducer exhibits a nonlinear relationship between its output voltage and measured displacement near the limit of its range. Therefore, tests were performed to characterize this nonlinearity. A cubic relationship between the output voltage and displacement was established and used in the subsequent experiments.

The measurement cart also contains an optical sensor for measuring the flatness of the I-beam track. The optical sensor is controlled by a separate computer. The computer controls the data acquisition rate, the sensitivity of the sensor, and the refresh rate associated with the optical sensor. The raw data

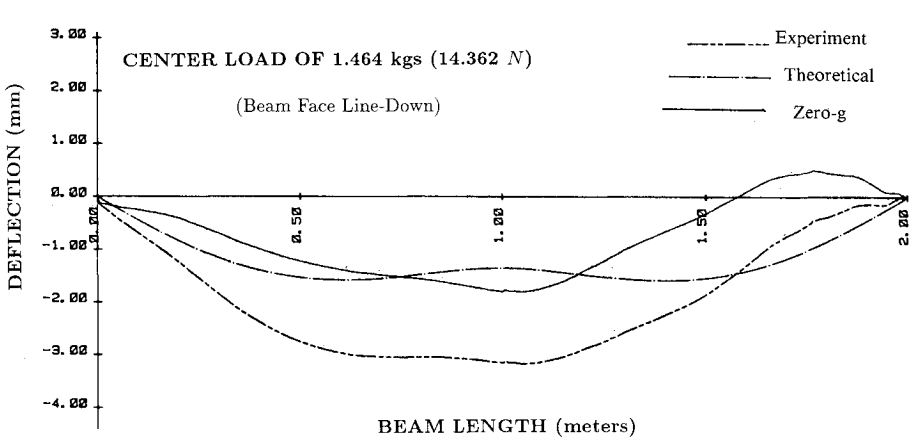

Fig. 8 Data from experiment 8.

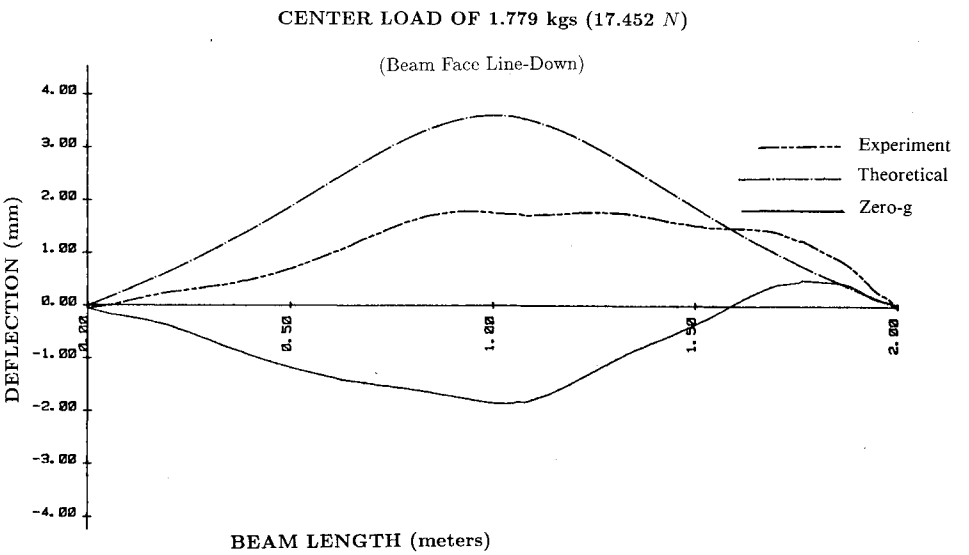

Fig. 9 Data from experiment 12.

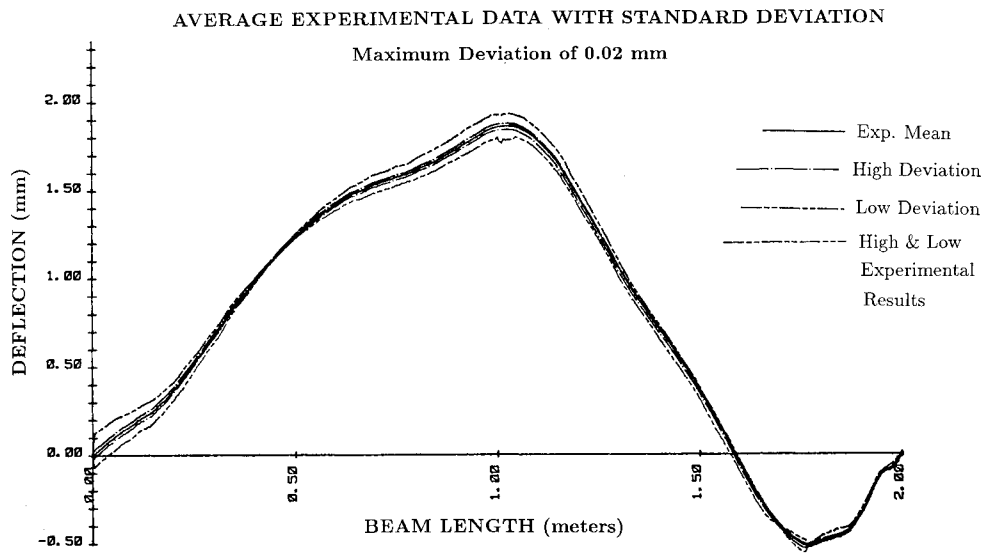

Fig. 10 Zero-*g* shape of experimental model.

are stored and then processed, from which the flatness of the I-beam is determined. A Micro-D camera assembly comprises the major part of the optical sensor.

The measurements of the force transducers, displacement transducer, and optical sensor are combined to determine the 0-*g* shape of the beam model.

Support Beam Measurement

The use of a support beam on which the measurement cart rides introduces measurement error. Any variation in flatness of the support beam translates directly into the displacement transducer. Therefore, it is necessary to derive a method for measuring the flatness of the support beam across the 2-m length of the beam model.

The support beam is initially milled to within ± 125 μm (± 5 mils) of flat across its length, but a ± 25 μm (± 1 mil) accuracy is desired in the measurement of the 0-*g* shape of the beam model. In order to achieve this accuracy, an optical RAM chip sensor, described in the measurement section, with detection accuracy of ± 21 μm is employed. The optical sensor is light-sensitive with refresh-rate and light-sensitivity controls. This allows the sensor to operate similar to a camera with aperture and film speed controls. At 51 positions along the beam model's length, images of a laser beam are taken in order to determine the support beam's shape.

A ± 200-μm laser beam is directed parallel to the measurement cart's path providing a horizontal reference. An optical polarizer is located on the cart between the laser and sensor, which allows for focusing of the beam. Pictures of the laser beam are taken at 51 points with a stationary cart and are used to established the horizontal reference for the experiment. Two of these pictures may be seen in Figs. 4 and 5. Figure 4 is point 1, the farthest distance from the laser beam; Fig. 5 is point 51, the closest point to the laser. The vertical center of these images is used for the horizontal reference. A computer program calculates the vertical mean, which serves as the center, by weighting all exposed pixels the same. To verify the repeatability of the beam center measurement, 10 tests are run at points 1 and 51. The first standard deviation in the beam center measurement at the furthest point from the laser, point 1, was ± 20 μm (± 0.8 mil), and at the closest point, point 51, ± 3 μm (± 0.13 mil).

Five separate measurement runs are combined to determine the support beam shape. It is noted that the support beam has approximately a ± 75-μm (± 3-mil) deflection. The raw data are shown in Fig. 6, and the same data with its linear slope subtracted in Fig. 7. The data in Fig. 7 are fit with an 11th-order polynomial, as shown, using a least-squares criterion. Despite the noticeable and repeatable valleys at 1100 and 1500 mm, it is felt that, due to the cart's constant motion

during the experiments, a smooth curve fit would be a good approximation to the data. Therefore, the 11th-order curve fit is used in the experiment to account for the deflection of the support beam.

Experiments

A total of 13 experiments are performed with a variety of load conditions. Six of these experiments are with the beam faced up and the other seven with it face down. These will be referred to as "line up" for the face-up state and "line down" for the face-down state. Note, the only difference between the two faces of the beam model is a paint mark placed by the experimenters. The beam has one redundant support, the center load, which is varied from 1.38 (13.54 N) to 1.78 kg (17.36 N) over the span of the 13 experiments. Two objectives are pursued using the experimental data. The first is to measure the 0-g shape of the beam model using the measured stiffness properties of the beam and an analytical model of the beam. The other assumes that the 0-g shape of the beam model remains constant, from which the stiffness of the beam, EI, is determined from the experimental data.

Plots of several typical loading conditions are shown in Figs. 8 and 9. In each figure, the measured shape, theoretically predicted shape, and 0-g shape are plotted vs the beam model's length in meters. The measured shape plot takes into account the measurement of the support beam, the slope the measurement cart traverses, and nonlinearities associated with the displacement transducer. The measured shape of the beam model for each experiment varies dramatically due to the change in load conditions. Figure 10 combines the 0-g shape plots of all of the experiments with plots of the maximum and minimum 0-g shape, average 0-g shape, and the first standard deviation. The average maximum displacement is on the order of 1.85 mm, with an error of ± 0.02 mm. A maximum error of 0.07 mm (4%) in the measurement of the beam's maximum displacement is observed.

In addition to the determination of the 0-g shape, the beam stiffness can be determined from the same experiments. The calculation of the stiffness, EI, (Nm^2 or psi) of the beam model employs a minimum in rms error as its criteria. The beam is assumed to exhibit the same properties as a Bernoulli-Euler beam. This is consistent with the analysis used in the determination of the 0-g shape. The difference between the experimental and theoretical data of the two runs can be written as

$$EI(\overline{\omega_1} - \overline{\omega_2}) = L^{-1}(F_1 - F_2) \tag{13}$$

rewriting using different variables

$$EI(T_e(x)) = T_c(x) \tag{14}$$

where $\bar{\omega}_i$ are the measured shapes of the beam model, and F_i the measured forces in the supports. $T_e(x)$ denotes the experimental data, and $T_c(x)$ denotes the theoretically calculated data. Formulating this as an optimization problem, we have

$$\frac{\partial}{\partial(EI)} \int_0^{2m} \left(EIT_e(x) - T_c(x)\right)^2 dx \frac{\partial}{\partial(EI)} (\text{const}) \tag{15}$$

$$2EI \int_0^{2m} T_e^2(x)\, dx - 2 \int_0^{2m} T_c(x) T_e(x)\, dx = 0 \tag{16}$$

solving for EI

$$EI = \int_0^{2m} F_c(x) F_e(x)\, dx \Big/ \int_0^{2m} F_e^2(x)\, dx \tag{17}$$

Since we are dealing with a finite number of points, Eq. (17) is rewritten as

$$EI = \sum_{i=1}^{n} T_{ci}(x) T_{ei}(x) \Big/ \sum_{i=1}^{n} T_{ei}^2(x) \tag{18}$$

where n is the number of data points. A total of 392 data points are collected each experimental run. The first 10 points of the experimental runs and the last 10 points are eliminated from the calculation as a result of the numerical difficulties associated with dividing small numbers. Each experimental run for the line-up (line-down) cases are compared to one another. In the line-up configuration, there are 15 comparisons; for line-down, 21 comparisons are performed. This corresponds to six experiments with the line up and seven with the line down. Comparisons between the line-up and line-down experiments are shown in Table 4. The value of stiffness EI used in the 0-g shape measurements was 104.05 Nm^2. The calculation of the stiffness of the experimental model is summarized as

line down:	21 cases $\overline{EI} = 104.3 \pm 2.8$ Nm^2	($\pm 2.7\%$)
line up:	15 cases $\overline{EI} = 105.1 \pm 5.2$ Nm^2	($\pm 5.0\%$)
Total:	36 cases $\overline{EI} = 104.6 \pm 4.0$ Nm^2	($\pm 3.8\%$)

The 0-g shape and stiffness results comfirm that it is possible to measure 0-g properties of structures in an Earth environment. The 0-g shape of a beam model is measured to within $\pm 1\%$ of its maximum displacement with a maximum error of $\pm 4\%$. The stiffness of the beam model is also determined from experiments to within $\pm 4\%$ of its measured value.

Table 4 Calculating EI from the experimental data

Line down, Nm^2:

	Experiments						
	1	2	3	4	5	6	7
1	—	104.23	104.96	102.75	103.66	104.20	104.63
2		—	105.43	101.75	103.35	104.15	104.70
3			—	94.46	101.53	103.39	104.36
4				—	106.89	106.87	107.02
5					—	106.81	107.07
6						—	107.30

21 cases: $\overline{EI} = 104.3 \pm 2.8$ ($\pm 2.7\%$)

Line up, Nm^2:

	Experiments					
	8	9	10	11	12	13
8	—	110.50	107.75	108.93	104.40	105.62
9		—	103.83	107.78	101.88	103.96
10			—	111.63	100.87	103.90
11				—	92.54	100.11
12					—	113.03

15 cases: $\overline{EI} = 105.1 \pm 5.2$ ($\pm 5.0\%$)

Total 36 cases: $\overline{EI} = 104.6 \pm 4.0$ ($\pm 3.8\%$)

Conclusions

An approach for identification of the 0-g shape of a beam/column in a 1-g environment was developed. The determination of the 0-g shape employed a combination of

experiment and analysis. To validate this methodology, a prototype large space structure was scaled to a laboratory-size model. A series of experiments was performed on the laboratory model, verifying that the 0-g shape can be measured to within $\pm 1\%$ of its maximum displacement with a maximum error of $\pm 4\%$. The stiffness of the beam model, EI, was also determined accurately. Future research would include determination of the 0-g shape of a laboratory truss and a prototype truss structure.

Acknowledgments

The authors would like to thank Dr. Jay-Chun Chen and John Garba of the Jet Propulsion Laboratory for their assistance. This work was funded by the Jet Propulsion Laboratory and the California Institute of Technology through a President's Fund Grant. The research was performed while the first author was a Ph.D. student under Dr. Babcock.

References

[1]Hedgepath, J. M., "Accuracy Potentials of Large Space Antenna Reflectors with Passive Structures," *Journal of Spacecraft and Rockets*, Vol. 19, May-June 1982, pp. 211-217.

[2]Mikulas, M. M., Jr., "Structural Efficiency of Long Lightly Loaded Truss and Isogrid Columns for Space Applications," NASA TM 78687, July 1978.